IEEE Access
Multidisciplinary | Rapid Review | Open Access Journal

Received 17 February 2023, accepted 6 March 2023, date of publication 10 March 2023, date of current version 15 March 2023.

Digital Object Identifier 10.1109/ACCESS.2023.3255645

RESEARCH ARTICLE

Fault-Tolerant Control of Gas-Lifted Oil Well

OJONUGWA ADUKWU[1,3], DARCI ODLOAK[2], AND FUAD KASSAB JUNIOR[1], (Senior Member, IEEE)

[1]Department of Telecommunications and Control, University of São Paulo, São Paulo 05508-010, Brazil
[2]Department of Chemical Engineering, University of São Paulo, São Paulo 05508-010, Brazil
[3]Department of Industrial and Production Engineering, Federal University of Technology Akure, Akure 340110, Nigeria

Corresponding author: Ojonugwa Adukwu (ojonugwa.adukwu@usp.br)

The research was supported by the Petroleum Technology Development Fund (PTDF), Nigeria while the APC was paid for by Coordenação de Aperfeiçoamento de Pessoal de Nível Superior (CAPES).

ABSTRACT The gas-lifted system has inherent ability to hide the effect of fault hence the system can inject gas into the annulus and oil will still be produced even in the presence of fault of significant value. This however affects the optimal operation of the system and could move the system towards the undesirable casing-heading instability. Faults of step decrease in the valves coefficients in addition to limitation on the valve affect the optimal flow of the liquids through the system. We detect and isolate these faults using generalised likelihood ratio test (GLRT) and Dedicated observer scheme (DOS) respectively. The states of the system are estimated using extended Kalman filter (EKF). Model predictive control based fault-tolerant control is then implemented on the system by using the robustness property of the zone control MPC and limiting the input bound in the optimiser. Both passive and active fault-tolerant control (FTC) were used to improve oil production or stabilise the system. Passive fault-tolerant control (FTC) provides more robustness but it does not change oil production noticeably enough. Reducing the upper control bound ensures stability but production could decline. Increasing the controller cost that prioritises the input target increases production but it is prone to casing-heading instability.

INDEX TERMS Fault-tolerant control, gas lift, model predictive control, optimisation, dedicated observer scheme.

I. INTRODUCTION

Gas-lifted system control is designed with the assumption of nominal operation of the system. The constraints for the optimisation or the controller are based on the fully functioning valves and sensors. But due to the nature of materials transported through the valve such as hydrates, wax, asphatenes, oil, gas etc [1] and its location, faults occur in the values that tend to degrade the performance of the system or even make the operation of the system dangerous. This is in addition to the fact that all automated systems are prone to fault [2]. Optimal and safe operation of the gas-lifted system must therefore include fault tolerant control (FTC).

Fault-tolerant control is an approach to use a controller in ensuring that a given safety-critical system functions to satisfactory level in the presence of fault of a given magnitude [2]. FTC is implemented using either passive approach or active approach. Passive FTC, employs the robustness of controller without the need for model update or controller reconfiguration. Active FTC however apply accommodation or control reconfiguration based on knowledge of fault presence and the magnitude of the fault [3]. In general, any means where fault effect on the plant or controller parameters is considered during controller design and plant operation is taken as FTC [4].

Fault-tolerant control is applied to virtually all engineering systems susceptible to fault. An FTC application to a multi-rotor unmanned aerial vehicle (UAV) which uses sliding mode control rather than MPC was presented in [5]. While this was not implemented using MPC, it was however implemented on a nonlinear system similar to our gas-lifted system. Proportional retarded controller was used to implement FTC on a stochastic nonlinear system where the stability was achieved from lyapunov stability analysis in [6]. An application to the upstream sector is presented in [7] for a blowout preventer (BOP) system. A PID controller is used to

The associate editor coordinating the review of this manuscript and approving it for publication was Diego Oliva.

monitor the BOP status for fault detection with voting used to decide the redundancy implementation. An overview of tools for the analysis of various FTC scheme is presented in [8].

MPC exhibits inherent fault-tolerance capabilities hence its use in FTC which dates back to the 90's and now has wide applications in various industries [9], [10]. In [3], the fault-tolerant capacity of MPC was used to monitor flow through actuators valves in Barcelona sewage system. Both passive FTC and active FTC performance on the sewage system were compared with the active case as expected, performing better in the network. In [11] explicit MPC was used for low level control of fuel cell in power system. Faults that affect the compressor range of operation were accommodated by computing offline the control law that takes note of the fault effects on the compressor. The use of MPC for fault-tolerant control of a satellite system is presented in [12]. However, the use of MPC in the fault-tolerant operation of gas-lifted system is yet to be reported in literature.

MPC fault-tolerant control is implemented by combining an online fault detection and identification (FDI) unit with a supervisory unit. The supervisory unit informs the MPC on either to modify the objectives to take into account the fault effect or change the constraints to reflect the current limitations of the inputs [11]. This is however possible under the assumptions that: (a) the FDI unit is working reliably (b) the MPC prediction model can be updated automatically and (c) the MPC control objective can be left unchanged after fault occurrence [13]. In cases where the system states can be measured accurately, the FDI unit takes the plant input and output to analyse the fault and provide the supervisory unit with the fault magnitude and presence as in the case of sewer models state [3]. Where the state measurements are not reliable, the FDI unit is combined with estimation or filter unit to provide the fault information to the supervisory unit and also provide the MPC with updated state estimates as used in the satellite models in [12].

Optimal operation of gas-lifted system using nonlinear model predictive control (NMPC) with zone control for casing heading stabilisation was presented in [14]. This zone control NMPC has inherent FTC capabilities which were not considered in the article but obviously, the controller can accommodate fault of low magnitude while still keeping the system states in their zones. In the passive FTC, the gas-lifted system zones can be carefully selected to aid continuous flow of gas from the annulus to the tubing and the controller parameters selected such as to keep the system far from the zone boundaries in the event of minimal fault. In the active case, the zone control MPC can combine this robustness property with model adaption, constraint change and objective prioritisation to obtain better FTC performance.

The flow rate through the gas lift valves depends on the valve coefficients which is a lump parameter that determines the flow per unit pressure drop across the valve at constant temperature and density of the liquid. Faults in valve affect these parameters which are to remain constant when pressure drop is constant. The occurrence of cavitation and flash in addition to other sources of wears and tears in the gas-lifted system valves alter these gas lift coefficients hence change the controller internal model [15]. This change in valve coefficient can be modeled as step fault in the valve coefficient hence fault-tolerant control using MPC implemented for optimal operation of the system.

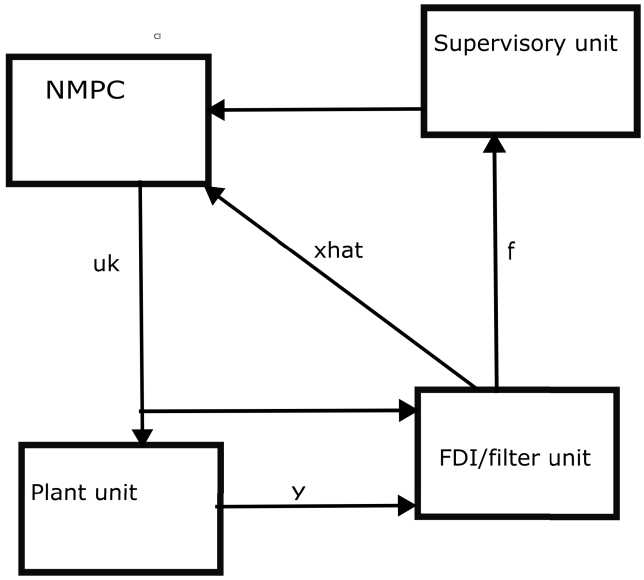

FIGURE 1. Schematic of fault-tolerant control (FTC). The fault diagnosis and identification (FDI) unit combines with the estimation unit to provide the supervisor unit with fault information and the NMPC with the estimated states.

In this article, we apply FTC in the optimal operation of gas-lifted system similar to [3] in sewage networks and [11] in fuel cell. The key difference between our work and these articles are: (a) use of an NMPC to increase operating points of our prediction model. (b) the FDI unit combines with state estimation to form the FDI/filter unit. While the estimator component of the FDI/filter unit provides the state estimates to the controller, the FDI component uses the state estimates to provide the supervisory unit with the health status of the system. (c) Passive FTC is applied to fault resulting from decrease in C_{pc} while active FTC is applied to faults resulting from increase in C_{pc}. (d) Gas-lifted system is a differential algebraic equation (DAE) system that is not straightforward to solve like the ordinary differential equation (ODE) system.

Fig. (1) shows the schematic of the FTC implemented in this article. The state estimation/FDI unit operates separately from the optimisation/control unit. The state estimation uses Extended Kalman filter (EKF) to provide the FDI sub-unit with the state estimates and also provides the MPC with updated state estimates [16], [17]. The EKF used here is presented in Apendix D while further details are found in [18]. The FDI uses generalised likelihood ratio test (GLRT) to detect fault and estimate its magnitude [17]. When fault is detected, the supervisory unit of the system operation determines the next operation. This action is either to change the upper bound of the valve constraints or alter the objective function priority in the controller. This takes advantage of MPC ease of representation of faults. While model modification is used for representing process fault like change in valve coefficients, input constraints modifications are used for valve faults [19], [20].

This paper is organised as follows: Section II presents the preliminary discussions considering valve faults, GLRT, DOS, MPC and FTC. Section III presents the valve fault diagnosis. Section IV presents fault-tolerant control while section V concludes the paper.

II. PRELIMINARIES

This article deals with fault-tolerant control (FTC) for gas-lifted system with valve faults using model predictive control. The controller used is the NMPC presented in [14]. It is a zone control MPC with input target. Further details of zone control MPC can be found in [21] and [22]. A brief discussion of fault-tolerant control in gas-lifted system valves using nonlinear MPC is therefore presented in this section. Gas-lifted system description is detailed in [23]

A. VALVE FAULT

Fault is an uncommitted deviation in the characteristics of all or a part of the system making the system unable to perform its function satisfactorily. Fault diagnosis involves three activities: (a) fault detection: detecting the occurrence of a fault, (b) fault isolation: identifying faulty components and (c) fault identification: determining the magnitude and type of fault.

Valve faults could either be a stuck fault where the valve remains in one position irrespective of the control command, an outage fault when the valve delivers no input to the gas-lifted system or partial degradation where the performance of the valve decays with time. Partial degradation is considered as either a sudden change in the valve coefficient leading to an abrupt fault, a gradual change in the valve coefficient leading to a ramp/incipient fault or impulse in the coefficient.

Faults in valve include: valve clogging, positioner supply pressure drop, fully or partially opened bypass valve, flow rate sensor fault, internal leakage, stem displacement fault [24]. Some of these faults such as valve clogging, positioner supply pressure drop etc can have a jump effect on the flow rate. Also the occurrence of cavitation and flashing degrade the performance of control valves [15]. In deriving flow rate equation in gas-lifted system, all the constants that affect the flow rate through the valve are lumped together as the valve coefficients. For the flow through the injection valve, the C_{iv} is seen as the flow rate per unit pressure change (P) and percentage valve opening at a given temperature for a fluid of fixed density. Consequently, the flow rate through the valve is controlled by the coefficient and the percentage valve opening if the pressure, density and temperature are fixed. Similarly, fault affect the control of flow rate using the parameter, C_{pc} which is the production valve coefficient.

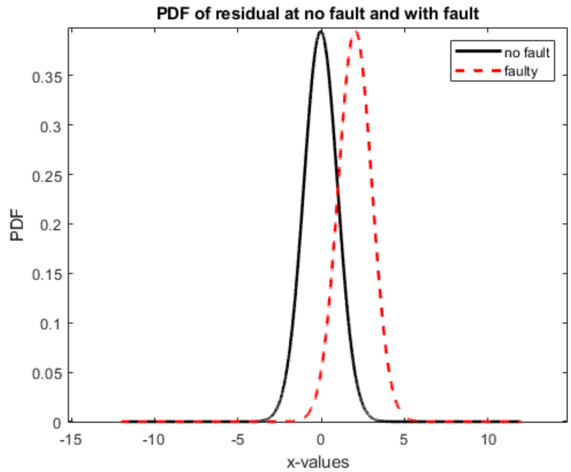

FIGURE 2. PDFs of residuals of faultless and faulty system. The presence of fault caused the mean of the PDF to change from zero to two.

These consequently affect the system dynamics that is purely determined by the flow rates. We therefore perform the fault diagnosis assuming these faults lead to a step change in the valve coefficient.

B. GENERALISED LIKELIHOOD RATIO TEST (GLRT)

The gas-lifted system considered here is noisy resulting from both measurement and process noise. A Gaussian noise assumption is made in this article. For our fault detection, we use the generalised likelihood ratio test (GLRT). The GLRT is a hypothesis testing algorithm for sequence of random variables whose parameter dependent PDF is suspected to have changed due to the change in parameter from a value θ_0 to another value θ_1, where $\theta_0 \neq \theta_1$. θ_0 is usually known and if θ_1 is unknown, the GLRT is employed to obtain a decision function. Using maximum likelihood estimator, the unknown parameters can be estimated and the method of CUSUM can then be used. But if θ_1 is known, the cummulative sum (CUSUM) approach is employed in obtaining the decision function to detect the change in the random sequence [25].

Fault has the tendency to change this parameter from θ_0 to θ_1 as shown in Fig. (2). In Fig. (2), the residuals for the faulty and faultless cases have the same variance but the mean of the two cases differ. The presence of fault caused the mean of the residual of the system to change from zero in the no-fault case (dark solid) to 2 in the faulty case (red dashed). The GLRT for such change detection is based on the decision function given in (1) [26].

$$g(k) = (\frac{1}{2\sigma^2}) \max_{k-N+1<j<k} \frac{1}{k+j-1} \left[\sum_{i=j}^{k} (y(i) - \mu_0) \right]^2 \quad (1)$$

where k is the sample time, σ is the standard deviation of the faultless system, N is the window size and μ_0 is the vector of mean for the three parameters when fault is not applied. N must be selected such that the time between detection and occurrence of fault is less than N. Meaning if K_0 = time of fault occurrence, K_a is the alarm time (time in which the fault is detected) and N_f is the detection delay (the time interval between fault occurrence and alarm time), then:

$$K_0 = K_a - N_f, \tag{2a}$$

$$N_f \leq N \tag{2b}$$

This ensures that the window is large enough for occurrence and detection to take place. But N must be kept small to reduce the computational demand. Equation (1) could have been interpreted as finding the maximum from N variance obtained using $N, N-1, \ldots\ldots, 1$ samples over a given data sample N if the differences are squared first before summation and not the case of summation before squaring as above. The magnitude of change in the parameter resulting from the fault is estimated by:

$$\hat{\theta}(k) = \frac{1}{k+j-1}\left[\sum_{i=j}^{k}(y(i))\right] \tag{3}$$

The parameters in this case are the mean and standard deviation of the residual. But we assume the standard deviation is constant and the fault leads to a change in mean of the error distribution hence $\theta = \mu$ = mean of residual while $y(k)$ is the residual. Once the decision function is obtained, then the threshold is selected such as to maximise the mean time between false alarm and minimise the mean detection delay. These performance requirements are given as:

$$\hat{\bar{T}}_D = \bar{L}(\mu_s), \tag{4a}$$

$$\hat{\bar{T}}_{fa} = \bar{L}(-\mu_s) \tag{4b}$$

where $\hat{\bar{T}}_D$ is the estimated mean time for detection and $\hat{\bar{T}}_{fa}$ is the estimated mean time between false alarm.

If σ_s is $\frac{(\mu_1-\mu_0)^2}{\sigma^2}$, μ_s is $\frac{(\mu_1-\mu_0)^2}{2\sigma^2}$, μ_0 is the mean of the residual distribution before change and μ_1 is the mean after change [17], [27]. L is defined according to [27] as:

$$L(\mu_s) = \frac{\sigma_s^2}{2\mu_s^2}(\exp\left[-2(\frac{\mu_s h}{\sigma_s^2} + 1.166\frac{\mu_s}{\sigma_s})\right] + 2(\frac{\mu_s h}{\sigma_s^2} + 1.166\frac{\mu_s}{\sigma_s}) - 1) \tag{5}$$

C. DEDICATED OBSERVER SCHEME (DOS) SYSTEM

The dedicated observer scheme shown in Fig. (3) for three output system applies one input to each observer while the observer estimates the entire output variables if possible. For a no fault situation, the estimates of an output variable from all the observers is the same and equal to the true output from the system. If however, the input to an observer is faulty, the entire output from the observer is erroneous. The observer however estimates the erroneous output (now input to the observer). The residual for the output variable that is the input to the given observer is zero while the residuals for the other variables are nonzero. While this scheme is capable of detecting multiple faults, it is only applicable to system in

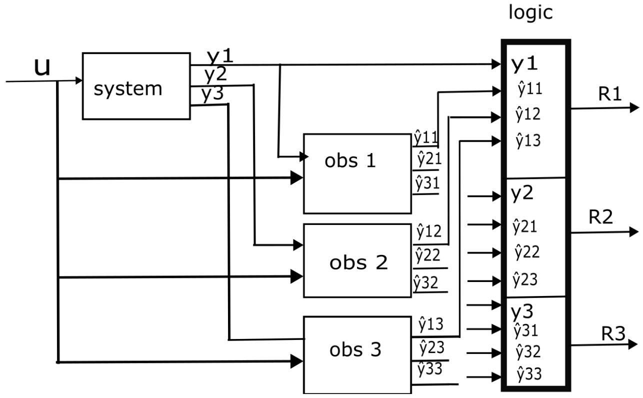

FIGURE 3. Dedicated observer scheme. In this fault isolation scheme, each observer is fed with one output of the system while the observer outputs the estimates of the three variables.

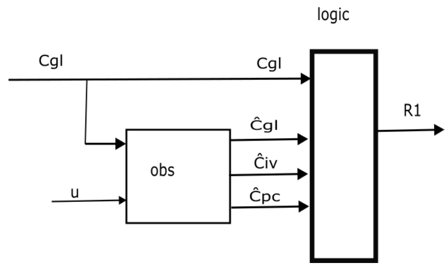

FIGURE 4. Logic unit. If C_{gl} is faulty, all the inputs to the logic unit will be erroneous. If C_{gl} is fault-less, all the inputs to the logic unit will be correctly estimated.

which the full states are observable or large part of the full states are observable. In the gas-lifted system presented, all the states are observable.

The logic unit in Fig. (3) determines if a variable is faulty or not by evaluating the residual using the true system outputs and the estimated outputs from the observers. The output of the logic unit indicates a fault in the given variable based on the algorithm employed. In this article, we treat the valve coefficients as the output variables. Observer 1 is fed with C_{gl}, observer 2 is fed with C_{iv} while observer 3 is fed with C_{pc}. A fault in C_{gl} implies the estimates from observer 1 is erroneous while the estimates from observers 2 and 3 are accurate. The logic unit in Fig. (4) extracted from Fig. (3) for only C_{gl} shows the observer input as C_{gl} and providing the estimates for all the outputs. All these estimates are erronous if C_{gl} is faulty. Applying the logic discussed in section (3.3), the fault in C_{gl} can be isolated.

D. NONLINEAR MODEL PREDICTIVE CONTROL

Model predictive control (MPC) is a control algorithm that uses an explicit model of the system to be controlled to predict the state trajectory over a given horizon [28], [29]. MPC solves an online optimal control problem to obtain the optimal input sequence in (6). The close-loop control law is defined by only the first element of this optimal input sequence in (7). This control law could be different for faulty system and fault-free system. At the next sample time, the horizon recedes, new measurements are taken and the process is repeated thereby minimising the effect of not only the mismatch between predicted model and actual plant but also disturbances in the plant.

$$U_k = \left[u(k|k)^T, u(k+1|k)^T, \dots \right] \tag{6}$$

$$u_k = u(k|k) \tag{7}$$

MPC major features are the use of model, the multi-variable approach, the ability to incorporate constraints in its formulation, the receding horizon and the solution of the optimal control problem. The models are usually linear due to the fact that the resulting optimisation problem is convex hence global optimum are easy to be obtained. But research in nonlinear control that permits the use of nonlinear models now abound in the literature. The use of nonlinear model ensures that wide range of prediction horizon are realised at the expense of high computational cost and risk of not getting the global optimum [30].

MPC solves multiple objective function usually relating to state deviation from reference states, input moves, absolute inputs among others. The overall objective is the weighted sum of the individual objectives. Nonlinear MPC application to gas-lifted system is still very scanty. Nonlinear MPC is used by [31] for improving oil production using two inputs (choke valve and gas lift flow rate). Areas of MPC use in fault-tolerant control in gas-lifted system does not exist yet.

E. FAULT-TOLERANT CONTROL

Depending on the type and degree of fault, the system performance can change from satisfactory performance through degraded performance, unsatisfactory performance to danger regions as shown in (5) [17]. The objective of real time control of dynamical system is to operate the system in the region of satisfactory performance but the presence of fault makes the system performance move into any of the region of performance including danger region where it becomes catastrophic to operate the system.

While the presence of fault moves the system behaviour from satisfactory performance towards danger in Fig. (5), the function of FTC is the reverse. The acceptance of what constitutes each performance above depends on the system and the management decision. In the case of gas-lifted system, satisfactory performance could be stated in terms of the mean oil production relative to supplied gas. Degraded performance occurs when the mean production relative to gas supplied declined noticeably. The system enters unsatisfactory performance region when casing-heading instability sets in with its effects on the downstream equipment. The system enters danger zone if for example the faults causes much production beyond the capacity of the storage tanks due to adverse casing-heading instability.

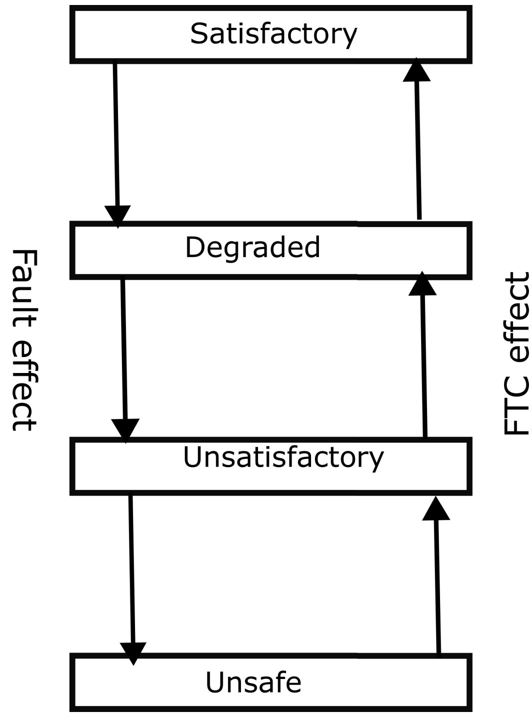

FIGURE 5. Fault and fault-tolerant control (FTC). While the fault moves the operation of the system from satisfactory performance to danger, FTC moves the system performance in the reverse direction.

III. VALVE FAULT DIAGNOSIS IN GAS-LIFTED SYSTEM

We augment the states of the system by including the valve coefficients as additional states variables hence our augmented states are defined as:

$$x = [m_{ga}\ m_{gt}\ m_{ot}\ C_{gl}\ C_{iv}\ C_{pc}]^T \tag{8}$$

The additional states are the valve coefficients given in Appendix C. They are described further in section III-A. These augmented states vary for m_{ga}, m_{gt}, m_{ot} but remain constant for C_{gl}, C_{iv} and C_{pc} until the arrival of faults.

A. PARAMETER DESCRIPTION

The process of fault detection starts from generating a residual signal, r. At steady state, this signal remains constant for every sample even in the presence of input and disturbance but changes due to fault presence only. In the stochastic case considered here we assume the noise to be Gaussian distributed hence the residual (innovation in this case) has zero mean with non zero variance in the absence of fault but a non zero mean at some or all points in the presence of fault. In selecting the parameters for the gas-lifted system to be used in generating this residual for the fault signatures, there is no clear one in this case other than C_{gl}, C_{iv} and C_{pc}. But other variables change in known way to faults in the valves. Fig. (6) shows an abrupt fault of step decrease of 10% in C_{iv} introduced at the 20th minute, C_{pc} introduced at the 40th minute and C_{gl} introduced at 60th.

In Fig. (6), a step fault in C_{gl} does not affect the performance of C_{iv} and C_{pc}. The same is true for any of the

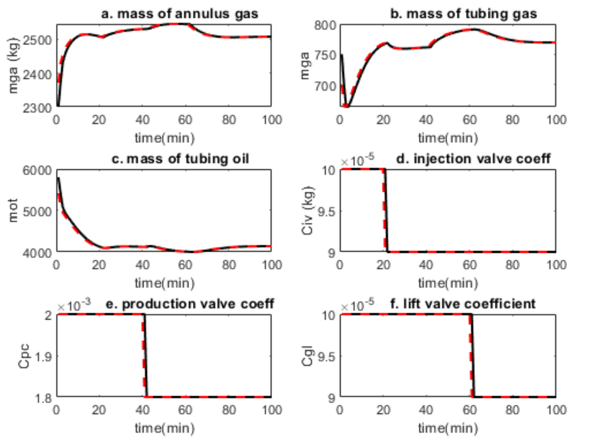

FIGURE 6. True and estimated states of the gas-lifted system. The true states are the dark continuous lines while the estimated states which are the red dash lines are the EKF outputs.

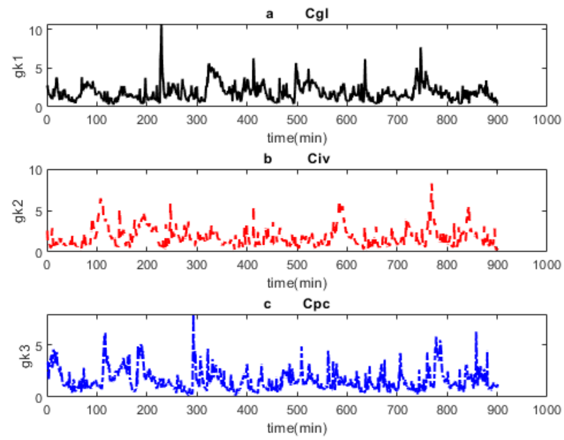

FIGURE 7. Generalised likelihood ratio test (GLRT): faultless case. The threshold can be approximated by selection of the maximum values for each residuals.

valve coefficients. Therefore, if a residual is generated for a fault in the C_{gl}, it will not affect the residual for the fault in the C_{iv}. Consequently, a strong detectability is ensured here.

Observe from Fig. (6) the increase in m_{ga}, a decrease in m_{gt} and an increase in m_{ot} at t = 20minutes corresponding to the time C_{iv} decreased. This is because a decrease in C_{iv} decreases flow from annulus into tubing hence increasing mass of annulus gas, decreasing tubing gas and increasing tubing oil due to reduced production. A decrease in C_{pc} implies low production through the choke. The mass of annulus gas increases since low production reduces flow from annulus to tubing, the mass of tubing gas increases and the mass of tubing oil increases. A decrease in C_{gl} decreases annulus gas mass, decreases tubing gas mass and increases mass of oil in tubing due to reduced production. The states therefore can also be used to generate residual for fault diagnosis purpose like the valve coefficients. Unlike the valve coefficients that remain constant under input change, the states can change due to input change as well as fault hence should only be used with the valve coefficients for residual generation.

B. HYPOTHESIS TESTING FOR FAULT DETECTION USING GLRT

The statistics of the residuals of the gas-lifted system change following the arrival of fault. It is the variation of the PDF with change in the residuals of selected parameters and variables that the GLRT discussed above rely through the formation of the log-likelihood ratio function of the residuals. The log-likelihoodhood ratio is the ratio of the PDF (evaluated at time k) of the residual after a change has occurred to the PDF before the change. If the value exceeds a given threshold, an alarm occurs indicating the presence of fault. Fig. (7) shows the GLRT function for the faultless gas-lifted system valve coefficients. It is seen that at no fault, these values are low.

The introduction of fault of reasonable value causes the values of the function to increase as seen in Fig. (8) for the case of a 20% decrease in valve coefficients occurring at 400th minute for C_{gl}, 500th minute for C_{iv} and 600th minute for C_{pc} respectively. In Fig. (8a), the fault in C_{gl} is difficult to be detected as the threshold may not be exceeded while it is much easier to be detected in Fig. (8b) but the GLRT function can fall below the threshold later. In Fig. (8c) however, the fault can be detected easily as the residual can be exceeded and never returned to.

Having discussed the GLRT, we present the hypotheses according to [27] as follows:

$$H_0 : \theta(k) = \theta_0 \qquad 1 \leq k \leq ct, \tag{9a}$$

$$H_1 : \theta(k) = \theta_0 \qquad 1 \leq k \leq k_f, \tag{9b}$$

$$\theta(k) = \theta_1 \qquad k_f \leq k \leq ct \tag{9c}$$

where k is the time instant, ct is the simulation time and k_f is the fault occurrence time. We select H_0 if there is no change in decision function above the threshold for the entire simulation time, otherwise, H_1.

If we approximate $\sigma_s = 2\mu_s$, then L for (4a) reduces (5) to (10a). Similarly, L for (10b) can be got in like manner, reducing (5) to (10b).

$$\hat{\hat{T}}_D = L(\mu_s) = 2\exp(-0.5h - 0.583) + h - 0.834, \tag{10a}$$

$$\hat{\hat{T}}_{fa} = L(-\mu_s) = 2\exp(0.5h + 0.583) - h + 3.166 \tag{10b}$$

Solving for h in (5) is very demanding computationally. A common approach used is the secant method. But [17] plotted the graphs of $\hat{\hat{T}}_D$ and $\hat{\hat{T}}_{fa}$ for various values of h and obtained the value of h that meets the desired performance considerations from the graph [17]. Here for each residuals we observe from the decision function plot in Fig.(7), select h that is greater than the maximum values for each of the residuals, then compute the performance from (10a) and (10b).

Equations (10a]) and (10b) increase with h but we desire that $\hat{\hat{T}}_D$ be small as possible while $\hat{\hat{T}}_{fa}$ be as large as possible.

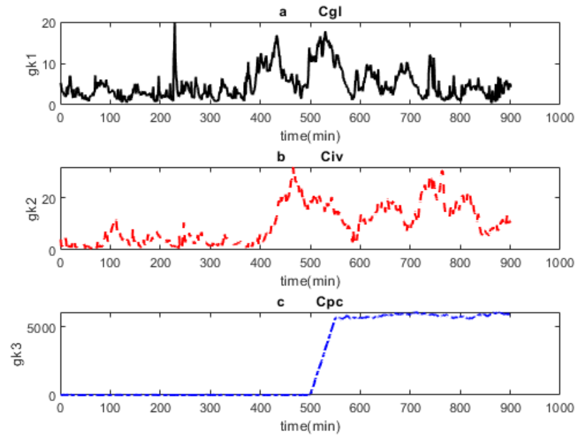

FIGURE 8. Generalised likelihood ratio test (GLRT): faulty case. Using maximum value as threshold makes the detection impossible for fault in C_{gl} while it is possible but difficult for C_{iv}. It is straightforward for C_{pc}.

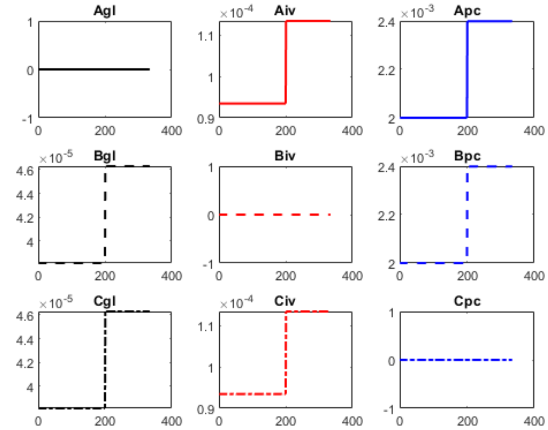

FIGURE 9. Residuals for gas-lifted system subjected to a fault of 20% step decrease in the valve coefficients. A_{gl}, B_{iv} and C_{pc} have zero values since the filter estimates for these variables agree with the true measurements.

Consequently, if we choose h based on Fig.(7), then vector of threshold is given as $h = [C_{gl}\ \ C_{iv}\ \ C_{pc}] = [11\ \ 9\ \ 8]$. The corresponding vector of mean detection delay and mean time between false alarm are $\hat{\hat{T}}_D = [10\ \ 8\ \ 7]$ and $\hat{\hat{T}}_{fa} = [869\ \ 316\ \ 191]$ respectively. Recalling that the time is in minute here implies that the detection delay for the production choke valve coefficient C_{pc} residual for example is 7 minutes which is desirable. However, the time between false alarm for C_{pc} residual is 191 minutes (3 hours) meaning regular occurrence of false alarms which is not desirable. With higher noise variance, $\hat{\hat{T}}_D$ is as high as 23 minutes which corresponds to a $\hat{\hat{T}}_{fa}$ of over a year which is desirable. Other factors can be used to choose the threshold in addition to the mean time between alarms and detection delay.

C. FAULT ISOLATION WITH DEDICATED OBSERVER SCHEME

We consider faults in the coefficients of the gas lift valves C_{gl}, the injection valve C_{iv} and the production choke C_{pc}. In the simulations, we select the outputs from the augmented states where the outputs are these valve coefficients. The observers are labeled A, B and C respectively. Based on the DOS described earlier, we apply only the first output C_{gl} to the first observer (observer A) while C_{iv} and C_{pc} are applied to observers B and C respectively. Fig. (9) shows the residuals for the gas-lifted system subjected to a step fault of 20% decrease in C_{gl}, C_{iv} and C_{pc}. A_{gl}, B_{iv} and C_{pc} correspond to residual of C_{gl} from observer A, C_{iv} from observer B and C_{pc} from observer C respectively.

The input to observer A is C_{gl} which is faulty starting at time t = 200 minutes. Observer A therefore produces wrong estimates of all the outputs. But since C_{gl} is also wrong, the residual (A_{gl}) becomes zero. Since C_{iv} and C_{pc} are not faulty, the corresponding estimates are nonzero implying A_{iv} and A_{pc} are nonzero. Similarly, for Observer B, B_{iv} is zero while B_{gl} and B_{pc} are nonzero. For Observer C, C_{pc} is zero while C_{gl} and C_{iv} are nonzero.

If we assign 1 to observer A, 2 to B and 3 to C, based on Fig. (9), the logic of the fault isolation can be given as: Variable i is faulty if 11 is true.

$$r_{ii} = 0, \tag{11a}$$

$$\prod_{i,j}^{m,n} r_{ij} \neq 0, i \neq j \tag{11b}$$

where a logical 1 (high) implies a fault in the residual and a logical 0 (low) implies no fault while m and n are number of outputs and observers respectively. Note that the product can only be high implying a fault in the variable or low implying no fault in the variable. Also the product in 11 for any variable excludes r_{ii} as indicated in 11a. A high is returned only when none of the residuals in the product is zero, it returns a low otherwise. Applying the logic in 11, a fault detected in section III-C is isolated as fault in gas lift valve coefficient (C_{gl}).

IV. FAULT TOLERANT CONTROL

After fault is detected and the effect is estimated, the next action is how to handle the effect of the fault so that the computed control law reflects the prevailing constraints due to fault presence while maintaining a level of production and preventing casing-heading instability. But if the magnitude of the fault is above a threshold, a more proactive measure other than control solutions are used following alarm. We consider three FTC cases here: (i) passive FTC, (ii) active FTC for increased C_{pc} and (iii) active FTC for reduced valve range fault.

A. PASSIVE FAULT TOLERANT CONTROL(PFTC) FOR REDUCED C_{pc} FAULT

In the passive case, there is no need for information from the FDI/filter unit during operation. The control zones are chosen offline such that the following objectives are met as far as possible:

(a) maintain the states in their zones at steady state.

(b) drive input towards the desired input target which will improve average oil production over open loop production.

(c) avoid casing-heading instability even if the system is operating at the input corresponding to unstable region.

(d) return the system to or close to the above after fault is detected.

The control zones are chosen based on the gas lift needs/limitations and the maximum/minimum values of the density obtained from simulations. In addition to this is the initial states that ensure the differential algebraic equation (DAE) has consistent solution. We note that the states which are masses depend on the density of the gas or mixture and the volume occupied. Based on the model and parameters values in the appendix, the volume of the annulus is calculated as 24.83 m^2 while that of the tubing is 17.25 m^3. The density of compressed annulus gas from simulation ranges between 57.84 kg/m^3 to 105.07 kg/m^3. These correspond to masses of 1436 kg and 2608 kg. It is desired to keep the minimum masses of gas in the annulus high hence keeping the annulus pressure high favouring constant flow of gas from annulus to tubing and reducing the chance of casing-heading instability. Therefore, we choose the minimum value of x_1 as 2000 kg while the maximum is 2600 kg.

From simulation, the density of mixture in tubing ranges between 50.82 kg/m^3 (at steady state with high gas content) and 800kg/m^3 (when filled with oil only). These values correspond to masses of 876 kg and 13799 kg respectively. Based on this and the initial solution to the DAE system, x_2 zone is taken as 350 kg and 800 kg while x_3 is taken as 5000 kg and 7000 kg. The upper bound for x_1 is strict for safety purpose and the lower bound is strict to enforce casing-heading instability removal. The lower bounds for x_2 and x_3 must be low enough to ensure bound for x_1 is achieved without infeasibility. The upper bounds are dictated by safety concern and the need to reduce the downhole pressure.

The controller parameters are chosen in similar way to meet the above objectives. In addition to this is that the controller parameters are chosen such that a large margin is provided for state zones in case of fault occurrence. Recall that if the lower bound of x_1 is not violated, casing-heading instability is minimised. Also if the upper bound of x_2 and x_3 are maintained, the downhole pressure will be lower favouring more flow of crude into the well.

From several simulation results, the controller parameters used for the PFTC are selected as: $m = 4$, $P = 200$, $Q_x = diag([1 \;\; 1 \;\; 1]\text{x}10^3)$, $Q_u = diag([1]\text{x}10^7)$ and $R_u = diag([1]\text{x}10^5)$, T=60 s or 1 minute. When at time t=130mins, there is a 50% decrease in C_{pc}, the chosen controller parameters ensure that the state zones are not violated. Fig. (10) shows the three states of the gas-lifted system. The dark solid lines are the optimal states while the red dash lines are the estimated states from the filter. The green dash lines are the states zones. Fig. (10d) is the zoomed portion of the mass of oil in tubing (x_3). Fig. (11) shows the input and output corresponding to Fig. (10).

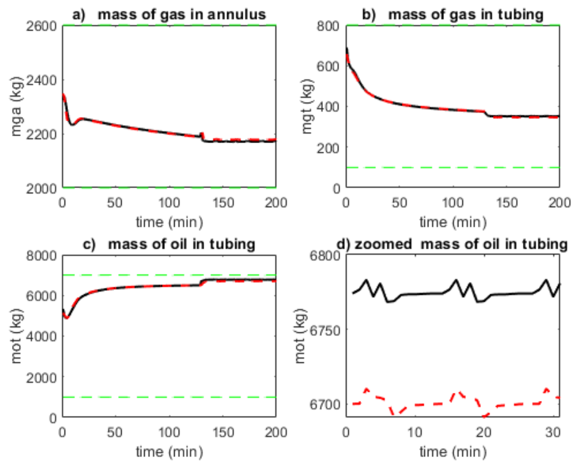

FIGURE 10. **States of gas-lifted system subjected to a fault of 50% decrease in C_{pc}.**

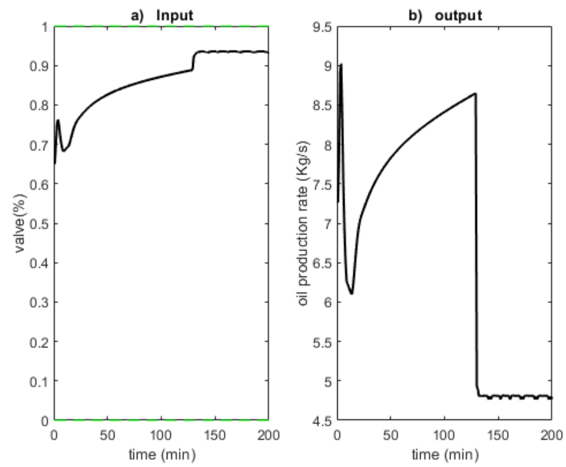

FIGURE 11. **Input and output of gas-lifted system subjected to a fault of 50% decrease in C_{pc}. The reduced C_{pc}, forces the controller to compute higher inputs but the production rate still falls below the nominal value.**

In Fig. (10), the state zones are respected despite the fault. The optimal states and the estimated states converged until the fault occurrence where they differ slightly showing the performance of the filter. Notice in Fig. (10d) that the zoomed portion of x_3 in the fault region shows slight disturbance and no real oscillatory behaviour. A decrease in Cpc implies a reduction of flow rate per unit percentage valve opening. This reduces rate of flow through the valve hence the controller computed higher values of the input as shown in Fig. (11a) where the input increases from 0.88 to 0.93 following the arrival of fault. The optimal production however declined from 8.7 kg/s to 4.8 kg/s as shown in Fig. (11b). When the same controller parameters were simulated for a fault of 50% increase in the C_{pc} and 10% decrease in the flow range, the corresponding flow rate due to these faults were 10.364 kg/s and 8.7104 kg/s respectively.

When higher priority was given to the deviation from the desired input, the rate of production increased but at the expense of oscillatory behaviour of the system. This scenario

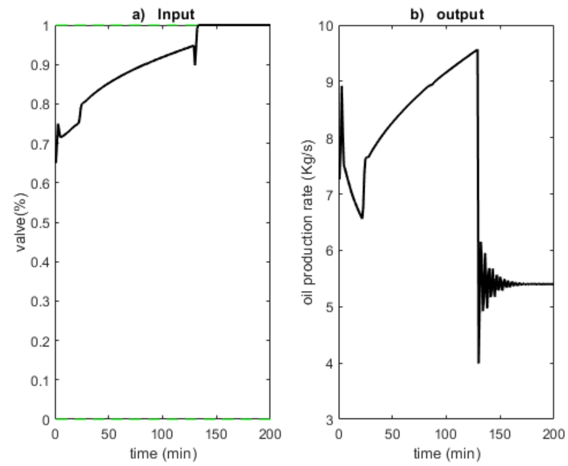

FIGURE 12. Input and output of gas-lifted system subjected to a fault of 50% decrease in C_{pc}. The increased control cost improves production but brought oscillatory behaviour.

is shown in Fig. (12) for $R_u = diag([1]x10^8)$. It is observed that the output increased to 5.4 kg/s compared to 4.8 kg/s in Fig. (11). However, oscillatory behaviour is experience especially at the beginning of the fault occurrence time. This oscillatory behaviour is not desirable in gas-lifted system [32], [33], [34]. This makes it difficult to attain higher production rate after fault occurrence using PFTC. Passive FTC does not depend on the reliability of the FDI/filter information hence the risk of poor performance due to wrong information is minimum, it is however conservative.

B. ACTIVE FAULT TOLERANT CONTROL(AFTC) FOR INCREASED C_{pc} FAULT

For a high magnitude of fault, active fault-tolerant control is preferred to passive FTC to increase production or minimise the occurrence of instability. If the fault magnitude is large but the optimisation in the controller does not result in infeasibility and the states are in their zones, fault accommodation is implemented by changing the upper bound of the constraints on the input to reflect the faults presence. If the upper bound for the nominal constraint is Ub_n, that of the faulty system is Ub_f and the magnitude of the fault is f, then the fault accommodation is implemented by defining the new constraint as in 12.

$$Ub_f = \begin{cases} Ub_n, & \text{if } f \leq 0 \\ Ub_n - f, & \text{if } 0 \leq f \leq a \\ a, & \text{if } f \geq a \end{cases} \tag{12}$$

where $0 \leq a \leq Ub_n$ which is the minimum constraint that will trigger operator intervention due to infeasibility of the optimiser.

This is represented in Fig. (13) where $a = 0.5$ and $Ub_n = 1$. A no fault report from the FDI/filter unit implies that the constraints remain unchanged while the constraint decreases linearly until it becomes 0.5 and remains constant thereafter. By this method, the fault in the production choke valve coefficient is accommodated. If however infeasibility results, or state zones are violated, human operator then decides the course of action as this is beyond the scope of this controller.

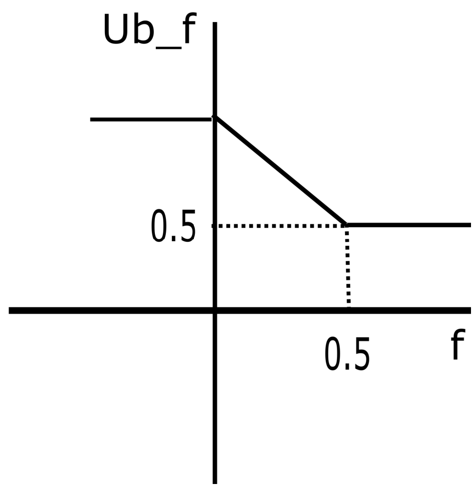

FIGURE 13. Modified constraint due to fault presence. The new constraint remains uncharged if there is no fault but decreases linearly with fault until 0.5 and remains constant afterwards.

Fig. (14) shows the gas-lifted system states with the same controller parameters as in the passive case above except the input target is now $R_u = diag([1]x10^8)$ as in Fig. (12) until a fault of 50% rise in C_{pc} occurs at time t=130 minutes. Fig. (15) shows the corresponding input and output. Despite an increase in C_{pc} means higher flow per unit increase in percentage valve opening, the controller tries to maintain high valve opening as shown in (15a). This value of input for the given C_{pc} resulting from fault makes the gas-lifted system go into casing-heading instability as seen in all the states in Fig. (14). The zoomed x_3 shown in (14d) shows the oscillatory behaviour resulting from the high input for the given C_{pc} more clearly. We avoid this casing heading instability by replacing the nominal upper bound constraint on the input with 13 to prevent the input from reaching the values that lead to infeasibility.

Fig. (16) shows the gas-lifted system states after the input constraints is changed due to information from the FDI/filter unit. Fig. (17) shows the corresponding input and output after the fault decreased the upper bound sharply to 0.8. The new constraint on the upper bound of the input caused the controller to compute an input that converged to the final value of the upper bound on the constraint as shown in Fig. (17a). The states in Fig. (16) are stable after fault occurrence. The increased value of x_1 helps to increase gas flow from annulus to tubing hence reducing chances of occurrence of casing-heading instability. This could however lead to build up of more gas in the tubing as shown in Fig. (16b) where x_2 increased after fault.

Due to the increased flow per unit percentage valve change, the production rate increased and saturated at 10.5 kg/s in Fig. (17b). In this case the fault leads to an increase in production rate and the active FTC leads to no instability. Note that such increased production has only temporal advantage as the valve might fail completely requiring replacement.

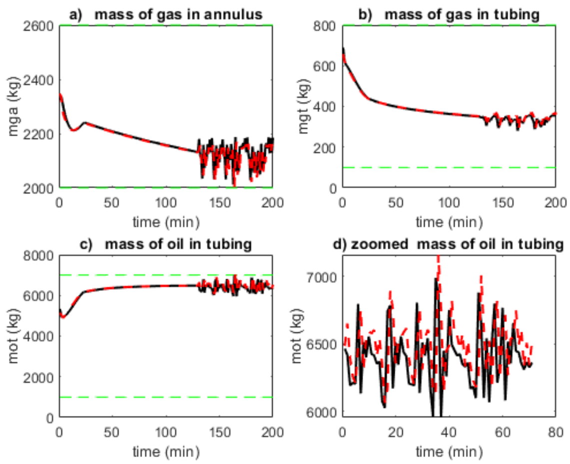

FIGURE 14. States of gas-lifted system subjected to a fault of 50% increase in C_{pc}. The increased C_{pc}, leads to casing-heading instability.

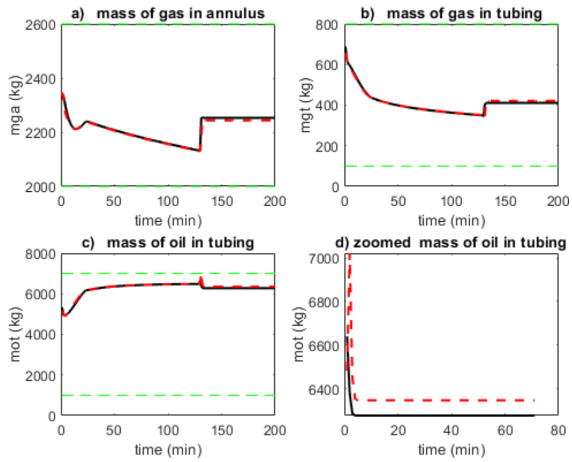

FIGURE 16. States of gas-lifted system subjected to a fault of 50% decrease in C_{pc} under active FTC. The reduced upper bound of the input stabilised the states.

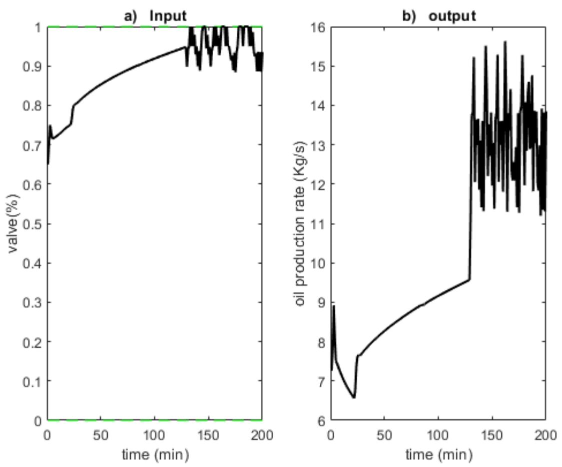

FIGURE 15. Input and output of gas-lifted system subjected to a fault of 50% increase in C_{pc}. Production increased but instability sets in.

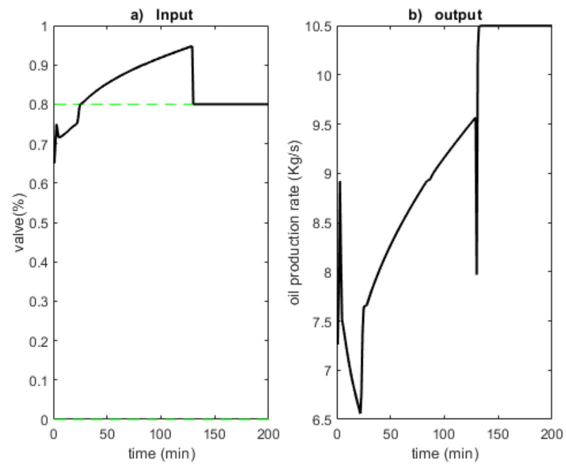

FIGURE 17. Input and output of gas-lifted system subjected to a fault of 50% increase in C_{pc} under active FTC. The valve constraints stabilises the output.

C. ACTIVE FAULT TOLERANT CONTROL(AFTC) FOR REDUCED VALVE RANGE FAULT

We now consider faults in valve that affects the flow range of the valve. Recall that fault in the valve coefficient modifies the internal control model while the fault in the flow range modifies the input constraint in the controller. In the case of a fault limiting the range of the valve, any FTC approach applied did not change the system response as the output remains constant at 8.7104 kg/s as shown in Fig. 18. This is because for any FTC approach used here, the input saturates at the upper limit of the input bound. Also the system does not show oscillatory behaviour of casing-heading instability for any FTC approach used.

D. COMPARISON OF FTC METHODS FOR VARIOUS GAS-LIFTED SYSTEM VALVE FAULTS

We compared the performances of various FTC techniques outlined above on the faults discussed. The performance criteria are (a) output change, (b) output and (c) stability. The output change for each FTC technique is the percentage change in output due to the application of a given FTC technique when fault occurs. This is obtained from the difference between the output after fault occurrence but before application of FTC (given in section IV-A) and the output after application of FTC. The faults considered are 50% decrease in C_{pc}, 50% increase in C_{pc} and 10% blockage of valve (or 90% upper limit of valve). The FTC techniques used are passive, change in input deviation weight Q_u in the controller and decrease in the constraints Ub_n on the input for the controller optimisation. The values for Q_u and Ub_n are chosen from nominal values that do not lead to casing heading instability.

Table 1 compares the performances of some FTC techniques for some valve faults using outpoint change from the output without FTC, output after FTC and oscillatory behaviour. From Table 1, for a 50% decrease in C_{pc}, the passive approach increases the output by 6.56% but there

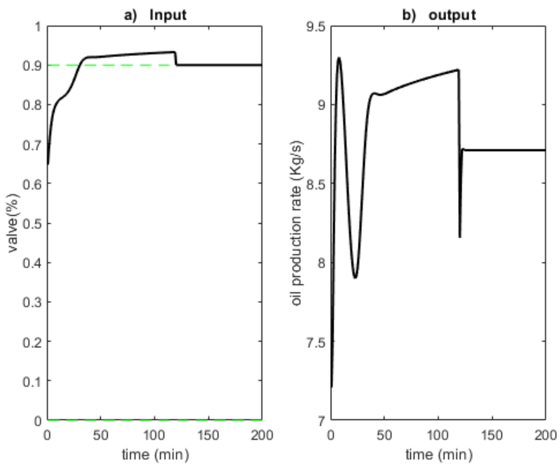

FIGURE 18. Input and output of gas-lifted system subjected to a fault of 10% decrease in valve range. Change in controller parameter does not alter the behaviour of the output.

was slight oscillation which damped out after a while. There was an oscillation when the input deviation weight in the controller was increased but the oil production increased also. Reducing constraints in the input leads to stability for any type of fault. Only in the case of 50% decrease in C_{pc} that instability is witnessed as there is no casing-heading instability when the fault is an increase in C_{pc} nor a 10% decrease in valve range. A fault of reduced control range of valve does not respond to any of the FTC techniques presented above since the change in output remains constant while there is no change in system stability. It however responds to model change involving change in the separator pressure (P_s) but this might not be realistic in practice.

Summarising the table above: Passive FTC provides more robustness but low output change. Reducing the upper control bound ensures stability but production could decline while increasing the controller cost that prioritises the input target increases production but it is prone to casing-heading instability.

E. ROBUSTNESS ISSUES WITH FTC METHODS FOR VARIOUS GAS-LIFTED SYSTEM VALVE FAULTS

So far we considered only noise in the states and output of the gas-lifted system which enabled the use of generalised likelihood ratio test (GLRT) for the fault detection. The gas-lifted system is also subjected to model uncertainty as most parameters are not constant as assumed in the model used above.

A key parameter of the gas-lifted system that changes hence altering the model of the gas-lifted system is the gas/oil ratio (GOR). This variation brings in model uncertainty as the flow rate of the reservoir gas (w_{rg}) depends on the value of the GOR (as shown in appendix A). This reservoir gas flow rate determines the size of the states particularly the mass of gas in the annulus (x_2). We therefore simulated the

TABLE 1. FTC techniques for some valve faults using outpoint change from the output without FTC, output after FTC and oscillatory behaviour. A yes under stability implies that there is no casing heading instability.

fault	FTC	output change (%)	output (kg/s)	stability
$0.5C_{pc}$	$Passive$	6.56	5.115	No
	Q_u	16.50	5.5918	No
	Ub_f	-11.61	4.2425	Yes
$1.5C_{pc}$	$Passive$	2.69	10.6425	Yes
	Q_u	16.50	11.0437	Yes
	Ub_f	-6.66	10.6423	Yes
$0.9Ub_n$	$Passive$	0	8.7104	Yes
	Q_u	0	8.7104	Yes
	Ub_f	-	-	Yes

system to examine the behaviour of the FTC schemes for a 20% increase and decrease in the GOR from the 0.01 value used. In all the cases, there was no noticeable change in the performance of the various FTC schemes.

In the passive FTC, the fault was accommodated for both the 20% increase and decrease in the GOR. This is due to the control zone selected for the NMPC used. In the selection of the zones, only the lower zone of the state x_1 is a priority as it helps to keep the mass of gas in that annulus at values that favours continuous flow of gas into the tubing. The lower zones of the other states can be chosen to be any positive value that will not result in infeasibility of the optimisation problem. This makes us select the zones that not only cope with state and output noise but also the change in the parameter.

In the active FTC, when the fault in the valve is an increase in Cpc, the change in the gas-lifted system model due to both increase and decrease in the GOR did nothing to the performance of the FTC. This is due to the fact that implementing the FTC by decreasing the upper constraint bound already causes the optimal input to converge to the upper bound of the input. Also in the active FTC involving limiting the valve range, the change in GOR could not affect the FTC scheme due to the saturation of the input at the upper bound of the input.

In summary, if they GOR is made to vary with 0.08 and 0.012 causing the model of gas-lifted system to vary, it will not affect the performance of the FTC schemes. While the selected zones helps to maintain the system in the zones in the presence of fault and model uncertainty, the saturation of the optimal control input to the upper control bound helps to cancel the effect of model uncertainty.

V. CONCLUSION

Fault-tolerant control (FTC) is used for optimal operation of gas-lifted system. Three cases were considered: (a) When a fault is due to a decrease in the production choke coefficient, passive FTC is used to increase production but could not prevent oscillatory behaviour of the system. This passive FTC is accomplished by proper selection of the controller parameters that ensures the NMPC is robust to these faults. (b) For the case where the fault is due to increase in the production choke coefficient, active FTC is used to remove casing-heading instability. This involves changing the constraints of the input to reflect the faults thereby preventing the system from sliding into casing-heading instability while increasing oil production. (c) For the fault due to reduction in valve range, active FTC could not alter the output noticeably. The FTC approach was robust to model uncertainties when the model was varied using the GOR of the gas-lifted system. This robustness was enhanced primarily due to the zone controlled NMPC used which permits control objective to focus on the optimal input that considers the FTC when the states are in the zones. This is the key advantage of using the zone control MPC for fault tolerant control compared to the tracking MPC that dominates the literature.

APPENDIX

A. GAS LIFT MODELS AND DEFINITIONS

For our FTC problem here, we use a slight modification of the models presented in [1] which were verified in OLGA software to be very close to the real system. These models are presented below: The definitions of the variables given in Table (2) while the parameters and the values are presented in Table (3).

The mass (differential equations);

$$\frac{dx_1}{dt} = w_{gl} - w_{iv} \quad (13)$$

$$\frac{dx_2}{dt} = w_{iv} + w_{rg} - w_{pg} \quad (14)$$

$$\frac{dx_3}{dt} = w_{ro} - w_{po} \quad (15)$$

flow rate;

$$w_{iv} = C_{iv}\sqrt{max(0, \rho_a(P_a - P_w))} \quad (16)$$

$$w_{pc} = C_{pc}\sqrt{max(0, \rho_t(P_{wh} - P_s))}f(u) \quad (17)$$

$$w_{ro} = C_{iv}\sqrt{max(0, \rho_0(P_r - P_{bh}))} \quad (18)$$

$$w_{pg} = \left(\frac{x_2}{x_2 + x_3}\right) w_{pc} \quad (19)$$

$$w_{po} = \left(\frac{x_3}{x_2 + x_3}\right) w_{pc} \quad (20)$$

$$w_{rg} = GORw_{ro} \quad (21)$$

The pressure;

$$P_a = \left(\frac{T_a R}{V_a M_w} + \frac{gL_a}{V_a}\right) x_1 \quad (22)$$

$$P_{wh} = \frac{T_t R}{M_w}\left(\frac{x_2}{V_t - \frac{x_3}{\rho_0}}\right) \quad (23)$$

$$P_w = P_{wh} + (x_2 + x_3)\frac{g}{A_t} \quad (24)$$

$$P_{bh} = P_w + \rho_0 g H_{bh} \quad (25)$$

Density;

$$\rho_a = \frac{M_w}{T_a R} P_a \quad (26)$$

TABLE 2. Lists of symbols, definitions and units of the variables used in the models.

Variable	Definition	Unit
w_{gl}	Gas flow rate into the annulus	kg/s
w_{iv}	Gas flow rate from annulus into tubing	kg/s
w_{rg}	Gas flow rate from reservoir into tubing	kg/s
w_{pg}	Gas flow rate through the choke	kg/s
w_{ro}	Oil flow rate from reservoir into tubing	kg/s
w_{po}	Oil flow rate through the choke	kg/s
w_{pc}	Mixture flow rate through the choke	kg/s
P_a	Annulus pressure	N/m^2
P_{wh}	Wellhead pressure	N/m^2
P_w	Tubing pressure	N/m^2
P_{bh}	Bottomhole pressure	N/m^2
ρ_a	Annulus gas density	kg/m^3
ρ_t	Tubing mixture density	kg/m^3

TABLE 3. List of the constants, definitions, units and values used in this article.

Parameter	Definition	Unit	Value
H_a	Height of annulus	m	1500
D_a	Diameter of annulus	m	0.189
H_t	Height of tubing	m	1500
D_t	Diameter of tubing	m	0.121
H_{bh}	Height of bottomhole	m	500
D_{bh}	Diameter of bottomhole	m	0.121
C_r	Reservoir valve coefficient	m^2	$2.6\text{x}10^{-4}$
C_{iv}	Injection valve coefficient	m^2	10^{-4}
C_{pc}	Choke valve coefficient	m^2	$2\text{x}10^{-3}$
ρ_0	Reservoir oil density	kg/m^3	1000
GOR	Gas/oil ratio	-	0.01
P_r	Reservoir pressure	N/m^2	$15\text{x}10^6$
P_s	Separator pressure	N/m^2	$2\text{x}10^6$
T_a	Annulus temperature	K	301
T_w	Tubing temperature	K	305
M_w	Molar mass of gas	kg	0.028
R	Gas constant	J/KM	8.314

$$\rho_a = \frac{x_2 + x_3}{V_t} \quad (27)$$

$$f(u) = 50^{u-1} \quad (28)$$

B. GAS LIFT VARIABLES DEFINITIONS

The variables in the derived formula and in the res of this article is given in Table(2).

C. PARAMETERS DEFINITION AND VALUES

The parameter values are presented here in Table (3). The parameters are also defined.

D. EXTENDED KALMAN FILTER

The extended Kalman filter (EKF) used for the estimation of the states for the fault diagnosis is described here briefly.

Consider the nonlinear discrete system presented in (29)

$$x_k = f_{k-1}(x_{k-1}, u_{k-1}, w_k), \quad (29a)$$

$$y_k = g_k(x_k, v_k) \quad (29b)$$

The state estimates for extended Kalman filter (EKF) follow similar pattern to the popular Kalman filter. For EKF however, prediction is preceded by finding the Jacobian matrices A and W. The update is preceded by finding the jacobian matrices C and V using the most recent state estimates. These matrices are used in the prediction and correction stages for the EKF. The most recent state during prediction is the recently estimated state at the immediate past sample time ($\hat{x}_{k-1}^{+}$). The most recent state during update is the just predicted state at the current sample time ($\hat{x}_{k}^{-}$). The state prediction however uses the nonlinear state transition function (29a) [18].

Pre-Prediction:

$$A_{k-1} = \left.\frac{\partial f_{k-1}}{\partial x}\right|_{\hat{x}_{k-1}^{+}}, W_{k-1} = \left.\frac{\partial f_{k-1}}{\partial w}\right|_{\hat{x}_{k-1}^{+}}, \tag{30a}$$

Pre-correction:

$$C_{k-1} = \left.\frac{\partial g_{k}}{\partial x}\right|_{\hat{x}_{k}^{-}}, V_{k-1} = \left.\frac{\partial g_{k}}{\partial v}\right|_{\hat{x}_{k}^{-}} \tag{30b}$$

The prediction and update procedure for the EKF is then given in (31) and (32) respectively.

Prediction:

$$\hat{x}_{k}^{-} = f_{k-1}(\hat{x}_{k-1}^{+}, u_{k-1}, 0), \tag{31a}$$

$$P_{k}^{-} = A_{k-1}P_{k-1}A_{k-1}^{T} + W_{k-1}Q_{k-1}W_{k-1}^{T} \tag{31b}$$

Correction:

$$K_{k} = P_{k}^{-}C_{k}^{T}(C_{k}P_{k}^{-}C_{k}^{T} + V_{k}R_{k}V_{k}^{T})^{-1}, \tag{32a}$$

$$\hat{x}_{k}^{+} = \hat{x}_{k}^{-} + K_{k}(y_{k} - g_{k}(\hat{x}_{k}^{-}, 0), \tag{32b}$$

$$P_{k}^{+} = (I - K_{k}C)P_{K}^{-} \tag{32c}$$

Equation (32b) is the estimated state of the system used for the fault diagnosis.

REFERENCES

[1] E. Jahanshahi, "Control solutions for multiphase flow: Linear and nonlinear approaches to anti-slug control," Ph.D thesis, Faculty Natural Sci. Technol., Dept. Chem. Eng., Norwegian Univ. Sci. Technol., Trondheim, Norway, 2013.
[2] M. Blanke, W. C. Frei, F. Kraus, J. R. Patton, and M. Staroswiecki, "What is fault-tolerant control?" *IFAC Proc. Volumes*, vol. 33, no. 11, pp. 41–52, 2000.
[3] C. Ocampo-Martinez, V. Puig, J. Quevedo, and A. Ingimundarson, "Fault tolerant model predictive control applied on the Barcelona sewer network," in *Proc. 44th IEEE Conf. Decis. Control*, Dec. 2005, pp. 1349–1354.
[4] E. F. Camacho, T. Alamo, and D. M. De La Pena, "Fault-tolerant model predictive control," in *Proc. IEEE 15th Conf. Emerg. Technol. Factory Autom. (ETFA)*, Sep. 2010, pp. 1–8.
[5] M. A. Ashraf, S. Ijaz, U. Javaid, S. Hussain, H. Anwaar, and M. Marey, "A robust sensor and actuator fault tolerant control scheme for nonlinear system," *IEEE Access*, vol. 10, pp. 626–637, 2022.
[6] S. Sweetha, R. Sakthivel, V. Panneerselvam, and Y.-K. Ma, "Nonlinear fault-tolerant control design for singular stochastic systems with fractional stochastic noise and time-delay," *IEEE Access*, vol. 9, pp. 153647–153655, 2021.
[7] X. Kong, B. Cai, Y. Liu, H. Zhu, C. Yang, C. Gao, Y. Liu, Z. Liu, and R. Ji, "Fault diagnosis methodology of redundant closed-loop feedback control systems: Subsea blowout preventer system as a case study," *IEEE Trans. Syst., Man, Cybern. Syst.*, vol. 53, no. 3, pp. 1618–1629, Mar. 2023.
[8] M. Blanke, M. Staroswiecki, and N. E. Wu, "Concepts and methods in fault-tolerant control," in *Proc. Amer. Control Conf.*, vol. 4, Jun. 2001, pp. 2606–2620.
[9] J. M. Maciejowski, "Modelling and predictive control: Enabling technologies for reconfiguration," *IFAC Proc. Volumes*, vol. 30, no. 27, pp. 19–29, Oct. 1997.
[10] J. M. Maciejowski, "Reconfiguring control systems by optimization," in *Proc. Eur. Control Conf.*, Brussel, Belgium, Jun. 1997.
[11] A. Rosich, V. Puig, and J. Quevedo, "Fault-tolerant constrained MPC of PEM fuel cells," in *Proc. IAR Annu. Meeting*, Nancy, France, Nov. 2006.
[12] D. A. Santos, "Fault-control state estimation of linear Gaussian systems subject to additive faults," Ph.D thesis, Aeronautic Inst. Technol., Brazil, 2011.
[13] J. M. Maciejowski, "Fault-tolerant aspects of MPC," in *Proc. IEE Seminar Practical Experiences Predictive Control*, 2000, pp. 1–3.
[14] O. Adukwu, D. Odloak, and F. K. Junior, "Stabilization of artificial gas lift system using nonlinear model predictive control with input target and control zones," in *Proc. IEEE Congreso Bienal De Argentina (ARGENCON)*, Dec. 2020, pp. 1–7.
[15] B. Ulanicki, L. Picinali, and T. Janus, "Measurements and analysis of cavitation in a pressure reducing valve during operation—A case study," *Proc. Eng.*, vol. 119, pp. 270–279, Jan. 2015.
[16] O. Adukwu, D. Odloak, A. M. Saad, and F. K. Junior, "State estimation of gas-lifted oil well using nonlinear filters," *Sensors*, vol. 22, no. 13, p. 4875, Jun. 2022.
[17] M. Blanke, M. Kinnaert, J. Lunze, M. Staroswiecki, and J. Schroder, *Diagnosis and Fault-Tolerant Control*, vol. 2. Berlin, Germany: Springer, 2006.
[18] D. Simon, *Optimal State Estimation: Kalman, H Infinity, and Nonlinear Approaches*. Hoboken, NJ, USA: Wiley, 2006.
[19] J. M. Maciejowski, *Predictive Control: With Constraints*. London, U.K.: Pearson, 2002.
[20] E. F. Camacho and C. B. Alba, *Model Predictive Control*. Berlin, Germany: Springer, 2013.
[21] A. H. González and D. Odloak, "A stable MPC with zone control," *J. Process Control*, vol. 19, no. 1, pp. 110–122, Jan. 2009.
[22] B. D. O. Capron and D. Odloak, "A robust LQR-MPC control strategy with input constraints and control zones," *J. Process Control*, vol. 64, pp. 89–99, Apr. 2018.
[23] Z. G. Xu and M. Golan, "Criteria for operation stability of gas-lift wells," SPE, Richardson, TX, USA, Tech. Paper 19362, 1989.
[24] S. K. Venkata and S. Rao, "Fault detection of a flow control valve using vibration analysis and support vector machine," *Electronics*, vol. 8, no. 10, p. 1062, Sep. 2019.
[25] A. Willersrud, M. Blanke, L. Imsland, and A. Pavlov, "Fault diagnosis of downhole drilling incidents using adaptive observers and statistical change detection," *J. Process Control*, vol. 30, pp. 90–103, Jun. 2015.
[26] A. Willersrud, L. Imsland, A. Pavlov, and G.-O. Kaasa, "A framework for fault diagnosis in managed pressure drilling applied to flow-loop data," *IFAC Proc. Volumes*, vol. 46, no. 32, pp. 625–630, Dec. 2013.
[27] M. Basseville and I. V. Nikiforov, *Detection of Abrupt Changes: Theory and Application*, vol. 104. Englewood Cliffs, NJ, USA: Prentice-Hall, 1993.
[28] J. A. Rossiter, *Model-Based Predictive Control: A Practical Approach*. Boca Raton, FL, USA: CRC Press, 2017.
[29] S. J. Qin and T. A. Badgwell, "A survey of industrial model predictive control technology," *Control Eng. Pract.*, vol. 11, no. 7, pp. 733–764, 2003.
[30] F. Allgower, R. Findeisen, and Z. K. Nagy, "Nonlinear model predictive control: From theory to application," *J.-Chin. Inst. Chem. Eng.*, vol. 35, no. 3, pp. 299–316, 2004.
[31] F. C. Diehl, C. S. Almeida, T. K. Anzai, G. Gerevini, S. S. Neto, O. F. Von Meien, M. C. M. M. Campos, M. Farenzena, and J. O. Trierweiler, "Oil production increase in unstable gas lift systems through nonlinear model predictive control," *J. Process Control*, vol. 69, pp. 58–69, Sep. 2018.
[32] G. O. Eikrem, L. Imsland, and B. Foss, "Stabilization of gas lifted wells based on state estimation," *IFAC Proc. Volumes*, vol. 37, no. 1, pp. 323–328, Jan. 2004.
[33] F. Scibilia, M. Hovd, and R. R. Bitmead, "Stabilization of gas-lift oil wells using topside measurements," *IFAC Proc. Volumes*, vol. 41, no. 2, pp. 13907–13912, 2008.
[34] A. P. Garcia, "Stability analysis and stabilization of gas lift systems," in *Proc. 22nd Int. Congr. Mech. Eng.*, 2013, pp. 3–7.

OJONUGWA ADUKWU received the B.S. degree from the University of Benin, Benin City, Nigeria, in 2006, and the M.S. degree from The University of Manchester, Manchester, U.K., in 2011. He is currently pursuing the Ph.D. degree in electrical engineering with the Escola Politécnica da Universidade de São Paulo (USP), São Paulo, Brazil.

From 2012 to 2014, he was an Assistant Lecturer with the Department of Mechanical and Biomedical Engineering, Bells University of Technology, Ota, Nigeria. He has been a Junior Lecturer with the Department of Industrial and Production Engineering, Federal University of Technology Akure (FUTA), Nigeria, since 2014. His research interest includes the application of model predictive control in the improvement of flow assurance in a gas-lifted oil well leading to the optimal operation of the systems.

DARCI ODLOAK received the B.S. degree from the Escola Politécnica da Universidade de São Paulo (USP), São Paulo, Brazil, in 1971, the M.S. degree from the Universidade Federal do Rio de Janeiro, in 1977, and the Ph.D. degree in chemical engineering from the University of Leeds, U.K., in 1980.

From 1991 to 1996, he was with Petrobras as the Head of the Advanced Control Group, where he developed and implemented an in-house advanced control package in the main oil refineries of Brazil. He has been a Professor with the Department of Chemical Engineering, USP, since 1987. He has more than 100 publications with over 2600 citations. He is the author of the book *Controle de Processos com Scilab*. His current research interests include robust model predictive control and the integration of control and real-time optimization.

FUAD KASSAB JUNIOR (Senior Member, IEEE) received the B.S. degree in physics and electrical engineering and the M.S. and Ph.D. degrees in electrical engineering from the Universidade de São Paulo (USP), São Paulo, Brazil, in 1985, 1989, and 1995, respectively.

From 1986 to 1988, he was a Consultant in industrial processes. He has been a Professor with the Department of Telecommunication and Control, USP, since 1988. He has more than 30 publications with over 200 citations. His current research interests include the modeling and simulation of dynamic systems, control theory, and optimization.